

P-MOSS: Learned Scheduling For Indexes Over NUMA Servers Using Low-Level Hardware Statistics

Yeasir Rayhan and Walid G. Aref
Purdue University, West Lafayette, IN, USA
{yrayhan,aref}@purdue.edu

ABSTRACT

Ever since the Dennard scaling broke down in the early 2000s and the frequency of the CPU stalled, vendors have started to increase the core count in each CPU chip at the expense of introducing heterogeneity, thus ushering the era of NUMA processors. Since then, the heterogeneity in the design space of hardware has only increased to the point that DBMS performance may vary significantly up to an order of magnitude in modern servers. An important factor that affects performance includes the location of the logical cores where the DBMS queries are scheduled, and the locations of the data that the queries access. This paper introduces P-MOSS, a learned spatial scheduling framework that schedules query execution to certain logical cores, and places data accordingly to certain integrated memory controllers (IMC), to integrate hardware consciousness into the system. In the spirit of hardware-software synergy, P-MOSS solely guides its scheduling decision based on low-level hardware statistics collected by performance monitoring counters with the aid of a Decision Transformer. Experimental evaluation is performed in the context of the B-tree and R-tree indexes. Performance results demonstrate that P-MOSS has up to 6 \times improvement over traditional schedules in terms of query throughput.

1 INTRODUCTION

NUMA and Heterogeneity. NUMA servers are heterogeneous in nature leading to varying cache and memory access latencies across sockets. For example, the inter-core latency across sockets in Intel Skylake X [26] can be 3 \times higher. Over the years, this heterogeneity has extended to within the socket itself. Earlier NUMA Servers (e.g., Intel Skylake X [26]) that logically partition the cores within a socket into separate NUMA nodes introduce a 1.1 \times increase in random memory access latency for any inter-NUMA node communication. Intra-socket heterogeneity becomes more prominent in modern chiplet NUMA servers, e.g., AMD EPYC Milan [2], where the inter-core latency between two cores in different chiplets can vary up to 4 \times . Even for servers with a high core count that do not employ chiplet architecture or any logical partitioning, e.g., a 72-core NVIDIA GH200 Grace Hopper Superchip [48], the inter-core latency between distant cores can vary up to 1.5 \times .¹

MMDBMS Indexes in the NUMA Landscape. The memory scalability enabled by the NUMA architecture has driven the revitalization of Main-Memory Database Management Systems (MMDBMSs) [17] in the past decade. Indexes serve as one of the core components in an MMDBMS contributing more than 50% of the total database size [72]. An index facilitates faster lookups, range scans, and indexed joins, with DBMSs even supporting *index-only* query operators, e.g., *index-only* scans [55] and *index-only* query

plans [30], leading to a wide range of index designs in the literature. Though overlooked in the literature, in the context of NUMA servers, the data partitioning and the query scheduling policies over a main-memory index can significantly dictate the index’s performance. Figure 1 shows the performance of a B⁺-Tree [11] in three different NUMA architectures under the 50% read-write YCSB [12] workload. Each data point refers to a different query scheduling policy of the B⁺-Tree. It is evident that the same B⁺-Tree can exhibit different performance under different data partitioning policies. Even two policies with the same data placement but a different core scheduling strategy can yield very different performance (cf. \circ markers in Figure 1). Moreover, no one policy performs optimally across all the NUMA architectures (cf. \blacksquare markers in Figure 1).

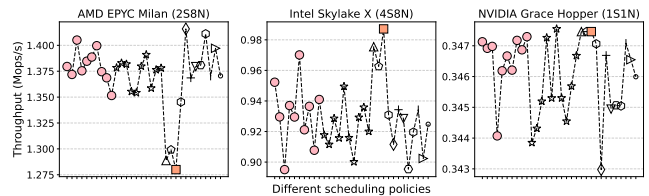


Figure 1: The performance gap of a B⁺-Tree under different scheduling policies can differ by upto 5.83 \times for different NUMA machines (§ 7.2).

Spatial Scheduling for NUMA. To this end, we introduce the notion of *spatial query scheduling*. This is orthogonal to the traditional query scheduling that is temporal in nature, i.e., when to schedule a query. In contrast, **spatial query scheduling explicitly decides which core in the underlying hardware gets to execute a query (compute selection), and which integrated memory controller (IMC) in the underlying hardware gets to store the data requested or generated by the scheduled query (data placement)**. Refer to Figure 2 for a complete overview of spatial scheduling. The core idea behind spatial scheduling is to keep the communication distance between two cores minimum to account for the intra-socket NUMA heterogeneity. The aim is to co-schedule queries that access common memory pages to nearby cores, while avoiding interference by scheduling interfering queries to distant cores. To account for the inter-socket NUMA heterogeneity, the goal is to strategically distribute data to appropriate IMCs and maximize local memory access, while ensuring that the full bandwidth of the memory channels and off-chip interconnects are utilized.

P-MOSS. In this paper, we introduce **P-MOSS**, a learned Performance Monitoring Unit (PMU)-driven Spatial Query Scheduling framework, that utilizes spatial query scheduling to improve the query execution performance of main memory indexes in NUMA servers. To accommodate larger indexes, P-MOSS *logically* partitions each index into multiple index *slices* based on the

¹All the numbers are generated on our testbed servers (See § 7).

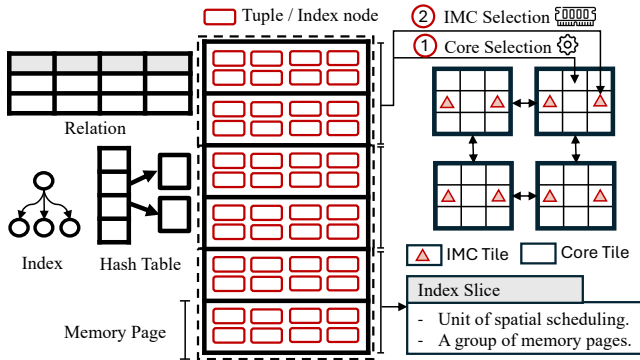


Figure 2: Spatial query scheduling.

index key, with each slice corresponding to a specific key range. These index slices serve as the unit of spatial scheduling. P-MOSS addresses the following question: **Given a main-memory index that is logically partitioned into multiple index slices on a NUMA server, how to find the best possible mapping for each index slice to a CPU core and a NUMA node, i.e., memory controller, such that the index performance, i.e., its throughput, is maximized.** To the best of our knowledge, P-MOSS is the first to address the problem of spatial query scheduling. Prior work, e.g., [38, 44, 53, 54, 57, 58, 61, 67], on query scheduling draws upon the temporal aspect of query scheduling, *partially* ([53, 54, 57, 58] only consider data placement in the context of relational tables) or *completely* ignoring its spatial aspect, and are orthogonal to the P-MOSS’s approach introduced in this paper.

P-MOSS’s Philosophy. P-MOSS follows a novel *Probe and Learn (PoLe)* technique. It involves probing the hardware during query execution to observe the hardware state under a given scheduling policy, and then gaining insights from multiple such hardware-DBMS kernel interactions to learn a better scheduling policy in an automated manner. At the core of this technique is the observation that any scheduling policy to speed up query processing is only as good as the traces the queries leave during their lifetime within the processor pipeline, e.g., the number of executed instructions, cache accesses, cache misses, stalled clock cycles, etc. PoLe treats these hardware statistics as a first-class citizen for optimization purposes, and aims to learn the inherent dynamics between a scheduling policy and the associated hardware statistics in a data-driven manner via Machine Learning to realize a robust and novel scheduling policy. This paves the way to design a generalizable framework across different hardware architectures and DBMS kernels under different data distributions and query workloads.

P-MOSS’s Driving Components. P-MOSS formulates the problem of spatial query scheduling as a Markov Decision Process (MDP) and adopts *Offline Reinforcement Learning* (§4.2) to learn the memory-page access and placement policies of an MMDBMS index. By adopting the offline RL scheme over the traditional RL, P-MOSS decouples the learning process from the DBMS kernel. This ensures that the DBMS does not under-perform during the learning cycle of the ML agent. Once the mapping policy of each index slice to the CPU cores and IMCs are learned, P-MOSS enforces the learned policy by localizing the query execution to the specific cores and distributing the memory pages over the mapped IMCs. The most noteworthy

aspect of P-MOSS is that the learning process is solely guided by the hardware performance statistics sampled by the *Performance Monitoring Unit (PMU)* [3, 5, 25] of the processor (§4.1), without any sort of bookkeeping. These statistics are the hardware traces left behind by the executed queries at different parts of the hardware, e.g., CPU cores, CPU caches, memory controllers.

Contributions. The main contribution of this paper is an architectural blueprint for a framework, P-MOSS, that is generalizable across diverse DBMS optimization tasks. P-MOSS requires no bookkeeping, and is adaptable across diverse hardware configurations, query workloads, and indexes. More specifically, the contributions of this paper are as follows:

- We introduce *P-MOSS*, a *learned query scheduling* framework over a main-memory index that prioritizes the spatial aspect of query scheduling, i.e., query execution and data placement, at the logical core and IMC levels.
- We develop DBMS kernel optimizations that are solely guided by the *low-level hardware statistics* collected by Performance Monitoring Units without any bookkeeping.
- We formulate the problem of query scheduling as a Reinforcement Learning (RL) problem, and adopt *Offline RL* that facilitates learning without requiring any online interaction with the DBMS.
- We perform an in-depth evaluation of P-MOSS for a diverse range of indexes (primary: B⁺-Tree, secondary: R-Tree), CPU vendors (Intel, AMD, ARM), NUMA hardware (1-4 NUMA Sockets, 2-8 NUMA Nodes), query workload, and report up to 6× throughput improvement over traditional scheduling.

2 P-MOSS’S DESIGN CONSIDERATIONS

We base the design principle of P-MOSS on the low-level hardware statistics collected from Performance Monitoring Unit of hardware, and Offline RL to realize the following design objectives.

Goal 1: The Need to Adapt to the Diverse CPU Vendors. In today’s hardware landscape, x86 (CISC) and ARM (RISC) are the most prominent processor architectures dominating the computing devices. IBM Power and RISC-v are notable alternatives. Intel and AMD are the leading manufacturers of x86 processors, whereas Apple, Amazon, and NVIDIA use ARM processors in their hardware. Generally, x86 processors have always had the edge over ARM in high performance computing with larger servers. In contrast, ARM processors dominate the smartphone, laptop, and desktop market as they consume less power, and have a reduced instruction set architecture. In recent times, ARM processors have become increasingly popular in servers, which begs the need for rethinking DBMS components for the ARM processors. Processors with the same architecture but from different vendors also exhibit distinct characteristics, e.g., Intel Skylake X distributes the L3 cache into slices across all the cores, whereas in AMD EPYC Rome, all cores in a Core Complex Die share a unified L3 cache. The same applies for the ARM processors built by different CPU vendors. Hence, a key goal of P-MOSS is to maintain robust behavior across diverse vendors, while adapting to its unique characteristics for optimal performance.

Goal 2: The Need to Adapt to the Ever Evolving Landscape of NUMA Architectures. The landscape of NUMA architectures is

always evolving, e.g., in earlier multi-socket NUMA servers, e.g., Intel Sandy Bridge, there is no localization within a socket, i.e., each NUMA socket has one NUMA node and one Integrated Memory Controller (IMC). This introduces excessive traffic on the memory channels for processors with high core count. To relieve the contention on the memory channels, later versions introduce more than one IMC in a single NUMA socket (e.g., Intel Ice Lake), and logically divide the cores, caches, and memory controllers into multiple NUMA nodes (e.g., Intel Skylake X). This introduces non-uniformity in the memory access latency even within a socket. The latest chiplet-based NUMA architectures, e.g., AMD EPYC Rome and Intel Sapphire Rapids, has further expanded this idea by physically assembling multiple chips inside a NUMA socket, and hence broadening the range of non-uniformity within a NUMA socket. AMD EPYC Milan and Rome have abandoned the use of IMCs in favor of a unified memory controller on a different chip. Hence, a key goal for P-MOSS is to adapt to these diverse NUMA architectures.

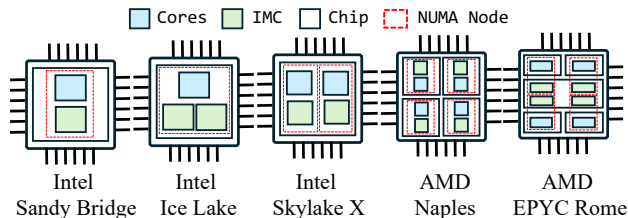


Figure 3: The socket layout of various NUMA architectures.

Goal 3: The Need to Handle Heterogeneous Query Workloads.

DBMS workloads are diverse, e.g., OLTP vs. OLAP at the applications level. Similarly, at the *hardware level*, workloads vary greatly in terms of their compute vs. memory accesses. The number of data requests generated by a lookup query served by a main-memory index is very small compared to a range scan, where the number of data requests can be very large depending on selectivity. Depending on the size of the result generated by a lookup or a range scan, different queries also exhibit different compute characteristics. A query executes a lower number of CPU instructions when the generated result size is small compared to when the result size is large. On top of that, query workloads are dynamic and can change frequently. For example, in scientific databases, the focus shifts from one data space to another on a daily basis for exploratory data analysis as new data is received periodically [20]. In such cases, the optimization needs to be swift and immediate. Thus, a key design decision for P-MOSS is whether to treat the diverse characteristics of the query workloads differently, and if so, how, while being swift.

Goal 4: The Need to Handle Conflicts. For optimal performance, the synergy between the DBMS, the OS, and the underlying hardware is necessary. However, there might be fundamental conflicts among their objectives. For example, the objective of the IMC is to ensure a higher DRAM throughput. Hence, it prioritizes sequential memory requests over random ones in its queue [14]. This contrasts with the objective of the DBMS, i.e., to ensure a higher query throughput. For DBMSs, prioritizing sequential memory requests over random ones will result in *interference* among concurrently running queries leading to a lower query throughput. For example, a lookup query may delay or starve due to a surge of concurrently running range scans. Similarly, the objective of the OS slab allocator

is to allocate the least amount of memory space by reducing the memory defragmentation, not accounting for the data hotness. This may lead to both hot and cold data being packed together in the same memory page, and hence leading to sub-optimal performance, e.g., high TLB (Translation Lookaside Buffer) misses [64, 71]. Hence, a key objective for P-MOSS is to keeping these conflicts between the DBMS, the OS and the hardware to a minimum.

Goal 5: The Need to Isolate the Learning Process from DBMSs in ML4DB Systems.

Reinforcement Learning (RL) has emerged as one of the more popular Machine Learning (ML) techniques in Machine Learning for Database (ML4DB) systems for building learned components, e.g., table partitioners [23], job schedulers [44, 61], knob tuners [40, 73], join order selector [33, 50], and query optimizer [45, 46]. These learned components fundamentally follow the *online* learning paradigm, termed Online RL, that requires the agent to actively interact with the DBMS, and collect experience based on the latest learned policy to improve upon itself. What distinguishes RL from other ML techniques is the concept of *exploration-exploitation*, i.e., the agent has to go through a continuous process of making mistakes, and progressively learning from these mistakes until it reaches a stable state. In the context of Online RL, this involves the agent taking sub-optimal decisions (actions) over a long period that may degrade the DBMS performance in an unpredictable manner. The exact same reason makes Online RL impractical for dynamic exploratory query workloads, especially when the span of the query workload is comparatively short. By the time an agent is optimized for a certain query workload, the workload has already changed, leaving the agent trapped in a never ending cycle of playing catch-up. Hence, it's of utmost importance that P-MOSS decouples the learning process from the DBMS operations.

3 OVERVIEW OF P-MOSS

Figure 4 presents the P-MOSS architecture. The key design principle of P-MOSS is to avoid any sort of application-oriented sampling [4, 64], and guide the learning process using only the PMU hardware statistics. Thus, it provides a general framework that can be abstracted across diverse hardware, query workloads, main memory indexes, or other DBMS optimization tasks. At the high level, P-MOSS can be decoupled into 2 main components: (1) the **system component** that handles the probing phase and (2) the **learned component** that handles the learning phase.

1. P-MOSS's System Component. The system component of P-MOSS is responsible for spatially scheduling the main-memory index. During query execution, P-MOSS periodically *probes* the hardware Performance Monitoring Units (§ 4.1), and generates a Hardware Snapshot of the index under the current scheduling policy. The Hardware Snapshot consists of hardware statistics from different parts of the hardware, i.e., CPU cores, memory controllers, and off-chip interconnect links. These hardware statistics are the bread and butter of P-MOSS, and go a long way in mimicking the data distribution and capturing the query workload. For example, a key range that is being queried extensively would result in a lot of cache and memory accesses. The number of cache accesses may further increase, if the data distribution within the key range is particularly dense. In the same spirit, a lookup query yields less cache and memory accesses compared to a range scan. Overall,

these hardware snapshots reflect the main-memory index state under the current scheduling policy from the perspective of hardware performance counters. P-MOSS periodically dumps the hardware snapshots to an offline dataset on which the learned component of P-MOSS is to be trained on.

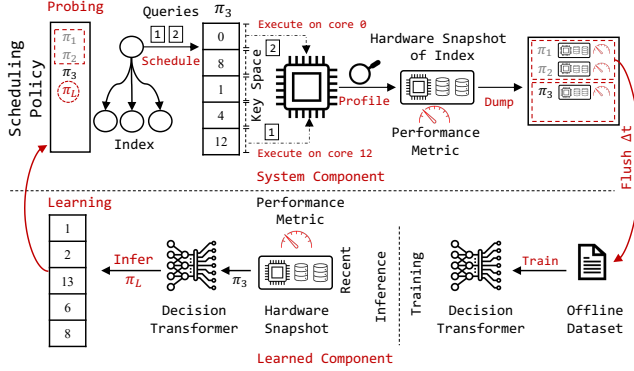


Figure 4: P-MOSS Architecture.

2. P-MOSS’s Learned Component. Recall that P-MOSS *logically* partitions the main-memory index into multiple index slices that serve as the unit of spatial scheduling. This requires no physical alteration of the index itself, rather a mapping of each index slice (key range) to a core and an IMC, i.e., the scheduling policy. And, this mapping is exactly what the learned component of P-MOSS learns. The learning process of P-MOSS is conducted *offline*, following the Offline RL (§ 4.2) paradigm. To learn a scheduling policy, P-MOSS’s learned component fully relies on the “offline” dataset. P-MOSS trains a Decision Transformer [10] (DT, for short) on the “offline” dataset in a supervised manner. Once the DT is trained on the “offline” dataset, the DT is fed the recent hardware snapshot(s) to infer a new learned scheduling policy. P-MOSS enforces the new core selection policy instantly, by updating the mapping between each index slice and the CPU cores. However, it rather takes a lazy approach in enforcing the new data placement policy. As the system component of P-MOSS accumulates new hardware snapshots, the learned component is trained to periodically update the spatial scheduling policy to ensure it remains up-to-date.

4 BUILDING BLOCKS OF P-MOSS

Before we move on to the details of P-MOSS, we present an overview of the Performance Monitoring Unit and Offline Reinforcement Learning, i.e., the two respective building blocks of the system and learned component of P-MOSS.

1. Performance Monitoring Units (PMU) Modern processors have dedicated hardware blocks throughout the chip, termed Performance Monitoring Unit (PMU, for short), that can track the hardware performance statistics [3, 5, 25]. These PMUs serve as the building block of P-MOSS’s system component. Almost all the hardware components, e.g., the cores, IMCs, interconnects, PCIe lanes of the processor are equipped with their own PMU blocks (cf. Figure 5). At the core of these PMU blocks, there are multiple counters (1 to 8 depending on the processor and the location of the PMU block) paired with a control register. Also, each PMU provides a fixed list of Performance Monitoring Events. Depending on the location of the PMU (inside or outside a logical core), these events

are classified into core and uncore events. Some of the counters are reserved to collect architectural monitoring events, i.e., events that behave consistently across hardware micro-architectures, e.g., the number of executed instructions, the number of LLC misses, the number of core cycles. The remaining counters can be programmed to monitor a single or multiple (through multiplexing) Performance Monitoring Events through the control registers.

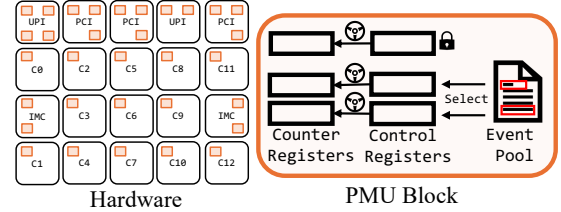


Figure 5: A high level illustration of Performance Monitoring Units (PMU) in modern processors. Note that, for brevity, we only show a selected number of PMU units.

2. Offline RL Offline RL serves as the building block of the learned component of P-MOSS. In Offline RL [39], the agent is provided with an offline dataset that consists of various state-action transitions. These transitions represent past experiences collected by running heuristic-based policies under different conditions. In P-MOSS, this offline dataset is a collection of Hardware Snapshots of the main-memory index. As the system component of P-MOSS runs the main-memory index under various scheduling policies for different query workloads and datasets, this dataset can grow overtime. The goal of offline RL is to learn a scheduling policy exclusively from this offline dataset, without any active interaction with the DBMS. This differs from the traditional RL setting, where the agent learns a new scheduling policy, and then deploys it in the real-world, i.e., into the DBMS for feedback. This can degrade the DBMS performance when the learned policy is sub-optimal. In contrast, there is no feedback loop between the agent and the DBMS in offline RL. The agent is constrained to learn only from the scheduling policies in the provided offline dataset. Hence, during the learning phase, P-MOSS’s learned component does not interfere with the DBMS. This presents the opportunity to train P-MOSS’s learned agent in a data-driven manner. Despite the difference in technique in how the agent learns a policy in offline RL, the goal of the agent still remains the same, i.e., to maximize a reward function, e.g., query throughput.

Why Choose PMU and Offline RL as the Building Blocks of P-MOSS? One of the key challenges of basing P-MOSS’s scheduling policy on PMUs alone is that the statistics collected from the PMUs can be non-deterministic, i.e., different runs can generate different values. However, the relative trends in these statistics remain consistent. Also, modern processors provide a large number of hardware events to profile. Hence, it becomes increasingly difficult to hand pick the important hardware statistics that fit across different NUMA architectures, query workloads, datasets, etc. On a similar note, the key challenges of employing offline RL in P-MOSS is: How to compile an offline dataset where the state-action transitions can abstract diverse CPU vendors, architectures, query workloads, and data distributions under a generalized framework? This is necessary so that the agent learns to generalize across these

different settings. Both PMU and Offline RL work in cohesion to address these challenges. The hardware statistics of PMUs can abstract across these diverse settings to generate high quality data and prepare an offline dataset. In the same manner, the ML techniques employed by the offline RL algorithms are well suited to handle the possible inconsistencies in PMU data as they focus on modeling the wider trends present in the data. Together, they guide the scheduling process in P-MOSS.

5 P-MOSS'S SYSTEM COMPONENT

Upon start, P-MOSS creates as many threads as the number of cores in the underlying hardware, and binds each thread to a core. Due to this, we use threads and cores interchangeably. In P-MOSS, each core in the hardware performs a diverse set of tasks ranging from routing, executing queries, to capturing hardware snapshots. Figure 6 illustrates the life of a query inside the system component of P-MOSS, where the numbers ① to ⑦ mark the chronological order of events.

① **Routing.** P-MOSS maintains a number of router cores that are distributed equally among the NUMA nodes. They route the incoming queries into the intended worker cores for execution. Each router core in P-MOSS maintains a copy of the scheduling policy. It evaluates the predicate of an incoming query to identify the index *slice*, i.e., the key range it belongs to, and uses the stored mapping to route the query to its destination core. If there are multiple cores to choose from (e.g., a range scan may overlap multiple key ranges), the query's destination core is chosen randomly to balance the load.

② **Query Execution.** Most cores in P-MOSS are worker cores that execute queries that involve traversing the index and producing results. Each worker core maintains two queues: a *job* and a *core stats* queue. A job queue stores the queries to be executed, and a core stats queue stores the hardware traces of an already executed query. The router cores are responsible for enqueueing queries into the job queue. A worker core dequeues one query at a time from the job queue, and executes it.

③ **Profiling Core HW Statistics.** Before the start of query execution, the worker core programs the *core* PMU counters of its PMU block to start profiling the compute, cache, and memory characteristics of the query. Once the query finishes executing, it stops profiling, and inserts the hardware trace of the query at the tail of the core stats queue. In P-MOSS, we profile the following core HW statistics for each worker core: clock cycles, instruction count, L1D (L1-Data), L1I (L1-Instruction), LLC (Last Level Cache), branch, memory, DTLB (Data Translation Lookaside Buffer), LLC-write, and memory-write misses, memory accesses, retired load instructions serviced from local and remote DRAM, cycles while L3 cache miss demand load is outstanding, and cycles while memory subsystem has an outstanding load. The granularity of the profiling can have an impact on system performance as it entails invoking kernel function calls. In P-MOSS, we set the granularity to 100, meaning that the hardware trace contains the cumulative core HW performance statistics of 100 executed queries.

④ **Profiling Off-core HW Statistics.** P-MOSS maintains a single off-core PMU sweeper core to collect the hardware traces left by a query in the *off-core* components, e.g., the memory channels, and the off-chip interconnects in the hardware. The off-core

components do not distinguish between the data requests they receive from the different cores, and hence, we cannot isolate these statistics on a per core (query) basis. Instead, we can collect these statistics at the NUMA node, or system level. In P-MOSS, the off-core PMU sweeper core periodically profiles the IMC and off-chip interconnect PMUs. Precisely, it profiles the bandwidth usage of each memory channel of the IMCs and the amount of incoming, outgoing traffic in the off-chip interconnects.

⑤ **Sweeping Round.** Each sweeping round, e.g., R0 includes sweeping the core HW statistics from each worker core, and sweeping the off-core HW statistics from the off-core PMU sweeper. P-MOSS maintains a core PMU sweeper core in each NUMA node. It sweeps the core HW statistics from the local worker cores, and creates a (partial) core snapshot of the corresponding NUMA node in the hardware. Similarly, the off-core PMU sweeper core creates the off-core snapshot of the hardware. Both the core and off-core snapshots are stored in the respective sweeper core's snapshot queue. To speed up the sweeping process, P-MOSS uses SIMD instructions extensively.

⑥ **Stitching.** P-MOSS has a core that periodically collects the core and the off-core snapshots from different sweeping rounds, and stitches them together to generate a complete Hardware Snapshot of the main-memory index under the current scheduling policy. Occasionally, the same core serves as the enforcer, and enforces a new learned scheduling policy. This involves migrating each index slice to its designated NUMA node, and updating the mapping policy stored in each router core. Recall that, in P-MOSS, each index slice logically maps to a key range. For a particular index slice, the migration is either performed aggressively by issuing a single migratory range scan over the entire key range, or lazily by issuing multiple migratory range scans over different portions of the key range. A migratory range scan migrates the index nodes that it touches to its destination NUMA node.

⑦ **Hardware Snapshot.** The Hardware Snapshot of a main-memory index comprises of the core HW statistics for each index slice and the system-wide off-core HW statistics. The hardware snapshot functions as the key input that guides the learning process of P-MOSS.

6 P-MOSS'S LEARNED COMPONENT

First, we discuss how P-MOSS formalizes the problem of query scheduling over a main-memory index as a Reinforcement Learning (RL) problem. Then, we discuss how P-MOSS's system component facilitates offline RL without interfering with DBMS operations. Next, we present the design of the Decision Transformer (DT) model that abstracts offline learning as a sequence modeling problem, and learns the scheduling policy in a supervised manner by conditioning on the desired objective, i.e., the query throughput.

6.1 Problem Setup

RL Problem Formulation. We take inspiration from the chip placement problem [35, 47], and cast the problem of spatial query scheduling over a main-memory index as a Reinforcement Learning (RL) problem, where the RL agent chooses each index slice one at a time, and sequentially schedules them on one of the worker cores. By default, we assume there exists an affinity between the core

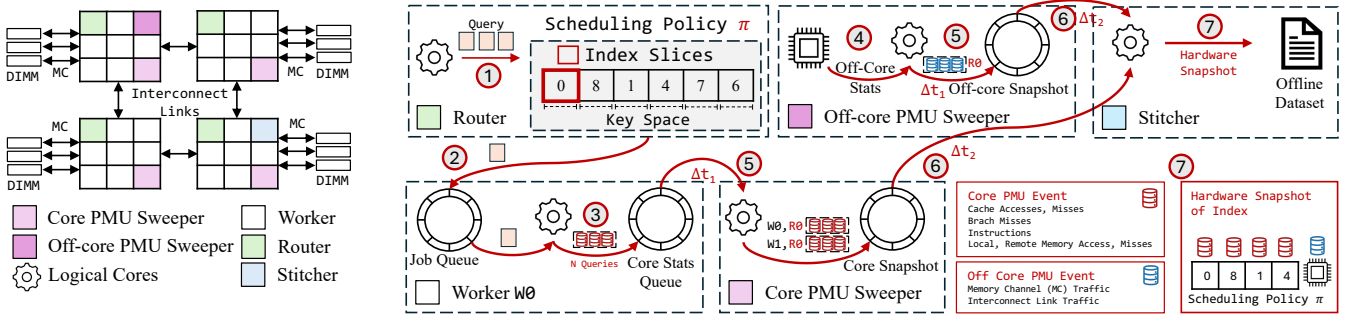


Figure 6: Life of a query inside P-MOSS's System Component.

and the NUMA node it is located in, in terms of data placement, to maximize local accesses. If an index slice is scheduled in a certain core, the index nodes within the slice are placed in the DIMM chip of the core's local NUMA node. Refer to Figure 7. At Time t_0 , none of the index slices are placed in the hardware. At Time t_1 , the agent places the first index slice into one of the free cores, say C4. This process continues until at Time t_T , the agent places the last index slice into Core C3. The non-worker cores (marked dark grey) are unavailable for the agent to choose from.

Agent-Environment Interface. Formulation of an RL problem is based on four elements denoted by the tuple $\langle S, \mathcal{A}, \mathcal{P}, \mathcal{R} \rangle$. We give an overview of these elements from the perspective of P-MOSS.

1. **State (S):** Given an MMDBMS index under a certain scheduling policy, P-MOSS uses the hardware performance statistics (e.g., instruction count, LLC misses) observed at different cores, the traffic in the memory channels and interconnect links, and the placement of the index slices on the hardware, to represent states of the DBMS index as well as the hardware.

2. **Action (\mathcal{A}):** Given the next index slice to schedule, the action space of P-MOSS constitutes of the worker cores that are feasible for the agent to choose from without any constraint violation.

3. **State Transition (\mathcal{P}):** Given the current state and an action, i.e., the scheduling of an index slice onto a core, how the current state transitions to a new state reflecting the aftermath of the latest placement. When the last index slice is placed, the agent reaches the terminal state.

4. **Reward (\mathcal{R}):** Once an index slice is scheduled into one of the worker cores of the hardware, the reward reflects how the stated decision improves the query throughput of the DBMS index.

Offline Dataset Creation. P-MOSS learns the query scheduling policy over the MMDBMS index *offline*, i.e., from a static dataset without active interaction with the DBMS. This is referred to as Offline RL. We collect a dataset $\mathcal{D} = \{\tau_1, \tau_2, \dots, \tau_D\}$.

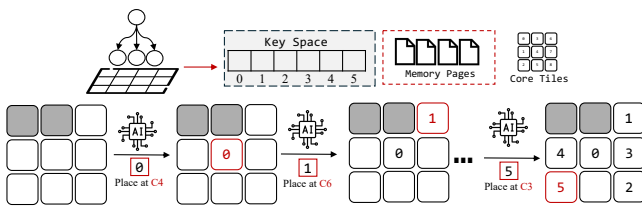


Figure 7: RL problem formulation of spatial query scheduling over a main-memory index.

Given a particular hardware, dataset and query workload, each $\tau = (\pi, \text{Hardware Snapshot}, \pi)$ in the dataset refers to a spatial query scheduling policy of the MMDBMS index and its hardware snapshot under the stated policy. Recall from Section 5 that it is P-MOSS's system component that provides the Hardware Snapshot of an MMDBMS index operating under a certain scheduling policy.

Figure 8 outlines the offline dataset curated for training the learned component of P-MOSS in the context of a B^+ -Tree for a particular hardware. The dataset reflects the B^+ -Tree state, i.e., how does the B^+ -Tree perform under varied spatial query scheduling policies for a given context, i.e., data distribution and query workload. Notice that the offline dataset does not maintain any information pertaining to the DBMS context. It only retains the Hardware Snapshot of the MMDBMS index that implicitly reflects both the DBMS context as well as the efficiency of the policy. Section 7 provides more detailed discussion of the datasets, query workloads, and the scheduling policies.

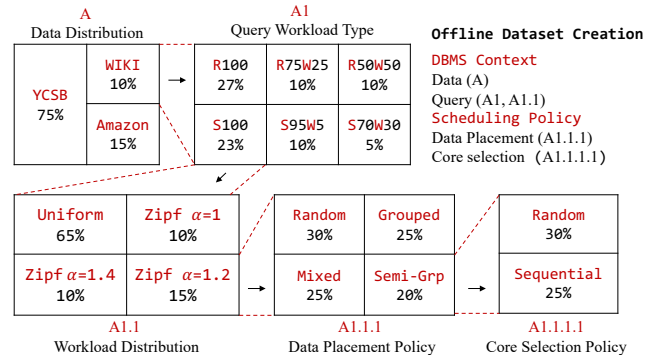


Figure 8: Offline dataset for a main memory B^+ -Tree. As the offline dataset grows, the percentages can vary.

6.2 Token Generation

Token generation is the first step in the overall pipeline of P-MOSS's learned component. In the *training* phase, P-MOSS traverses the offline dataset, selects each scheduling policy of the MMDBMS index along with its hardware snapshot, and generates the respective tokens pertaining to that scheduling policy. In the *inference* phase, P-MOSS rather collects the latest scheduling policy of the MMDBMS index and its corresponding hardware snapshot, then generates the respective tokens and feeds it to the trained RL agent for inferring the next scheduling policy. Refer to Figure 9 (Token Generation)

for the token generation process of an MMDBMS index scheduling policy π_1 , given its hardware snapshot.

1. State Token: State tokens represent the current state of the NUMA hardware given the latest (partial) spatial query scheduling policy. The state token in P-MOSS is generated by fusing three separate tokens: *view mask*, *position mask*, and *machine view*. Each of these tokens reflect the NUMA hardware state from a different perspective. P-MOSS represents the NUMA hardware as a $C_{m_i \times m_j}$ core tiles, where $|C_{m_i \times m_j}|$ refers to the total cores in the NUMA hardware. Each tile in $C_{m_i \times m_j}$ represents a single core with its associated components, e.g., cache, execution unit, etc. Only the worker cores in the NUMA hardware are eligible for scheduling. Cores reserved for routing or collecting hardware traces do not participate in the scheduling process. Next, we discuss each of these three tokens.

1a. View Mask. A view mask refers to the occupied core tiles in the NUMA hardware. It is a $C_{m_i \times m_j}$ tensor, where each entry represents if the corresponding core in the NUMA hardware has been scheduled to host any index slice or not. In Figure 9 (Token Generation), at Time t_0 , all the worker cores are empty as no scheduling decision has taken place yet. Hence, the view mask consists of all 0s'. At Time t_1 , the policy π_1 chooses Core C0 to schedule the first index slice. Hence, the corresponding entry of Core C0 in the view mask is set to 1. Note that, in P-MOSS, multiple index slices can be scheduled on the same core tile.

1b. Position Mask. A position mask refers to the worker cores that are eligible for the scheduling of the next index slice. It refers to a binary tensor, $C_{m_i \times m_j}$. Each entry in $C_{m_i \times m_j}$ with Value "1" means that the corresponding core is available for scheduling, whereas an entry with Value "0" means the corresponding core is not available. The non-worker cores are made unavailable for scheduling from the start, i.e., the corresponding entry is set to "0". Refer to the core tiles C3 and C5 in Figure 9 (Token Generation). These cores are made unavailable for scheduling from the beginning. The position mask can be used to impose further constraints on the scheduling of worker cores, e.g., ensuring that each worker core gets at least n index slices, or that the next index slice is placed in the vicinity of the previous index slice in the hardware, etc. P-MOSS does not impose such explicit constraints, i.e., each index slice can be placed in any of the eligible worker cores.

1c. Machine View. Machine view refers to the NUMA hardware state for a particular scheduling policy from the perspective of the *core* hardware counters. It refers to a $C_{m_i \times m_j \times H}$ tensor, H being the number of hardware statistics reserved for training the agent in a $C_{m_i \times m_j}$ core tile. In Figure 9 (Token Generation), the initial machine view at Time t_0 is empty. At Time t_1 , under Policy π_1 , the first index slice is scheduled into Core C0. Thus, the machine view is updated by aggregating the core hardware snapshot of the first index slice with the corresponding entry of Core C0. When multiple index slices are scheduled at the same core, the criterion to aggregate the hardware snapshots for the particular index slices can vary. P-MOSS has addition as the aggregation criterion.

2. Meta Token. The meta token refers to the NUMA hardware state for a particular scheduling policy from the perspective of the *off-core* hardware counters. Contrary to the *Machine View* token that represents the NUMA hardware state at the CPU core level, a meta token represents the hardware state at the system-wide level,

e.g., the state of the IMCs, off chip interconnects, etc. Aside from the off-core hardware snapshot of the MMDBMS index, the meta token includes the processor level information of the NUMA hardware, e.g., the number of logical cores, the number of NUMA nodes, and the number of sockets.

3. Action Token. The state space of the action token consists of all possible worker cores, i.e., Cores C0-C2, C4, C6-C8 in Figure 9 (Token Generation). At Time t_1 , as the first index slice is placed at Core C0, 0 serves as the action token for t_1 , then 8 for t_2 , etc.

4. return-to-go Token. The return-to-go token (RTG, for short) is calculated as the difference between the desired objective, i.e., throughput and the rewards observed so far. P-MOSS uses the DBMS's query throughput as the reward criterion for the RL agent. At Time t_0 , the return-to-go token is set to the maximum query throughput the DBMS targets to achieve, e.g., 10K (cf. Figure 9 (Inference)). As the index slices are placed sequentially one after the other, the return-to-go information is updated accordingly. At Time t_1 , the agent places the first index slice on Core C0 yielding a 2K throughput. As a result, the RTG for t_1 is updated accordingly to 8K.

6.3 Model Architecture

P-MOSS treats the offline RL problem of spatial query scheduling as a sequence modeling problem, and uses a Decision Transformer [10] to train the RL agent. A Decision Transformer (DT) [10] is an auto-regressive sequence model that predicts a future action based on the past observations conditioned on a return-to-go (RTG) token, and is built on top of the Transformer architecture [66].

Why Decision Transformer (DT)? There mainly exists three classes of offline RL algorithms, i.e., Q-Learning (e.g., [19, 31, 34]), Imitation Learning (e.g., [18]), and Transformer-based methods (e.g., [10, 74]). Each class has its own pros and cons. However, Q-Learning-based methods tend to suffer from instability and require extensive hyper-parameter tuning, while the Imitation-Learning-based methods require the policies in the offline dataset to be of very high quality. This makes these two approaches less appealing for use in P-MOSS. **The philosophy of P-MOSS revolves around relieving the DBMS kernel from hand-tuning scheduling policies through a learned agent**, thus spending considerable efforts in tuning the hyper-parameters of the learned agent is rather contradictory. Moreover, it is quite natural for the offline dataset to include sub-optimal policies, specially from the perspective of the DBMS scheduling. The reason is that no single scheduling policy can dominate across all query workloads, data distribution and NUMA machines (See §7). As the query workload, data distribution, or the hardware changes, the same scheduling policy is likely to yield sub-optimal performances. In contrast, Transformer-based methods can model very large sequences and are highly scalable. They also provide stable training, and greater generalizability that fits the desiderata of P-MOSS. In the context of RL for spatial scheduling, the number of index slices refer to the length of the sequence, and in P-MOSS, it is typically within [100, 1000]. Moreover, P-MOSS uses a large number of hardware counter statistics, typically in the range of [16, 48], and strives for generalizability across different CPU vendors, NUMA architectures, workload, and MMDBMS indexes. Hence, Transformer-based methods are particularly appealing to P-MOSS, and hence, we adopt DT in P-MOSS.

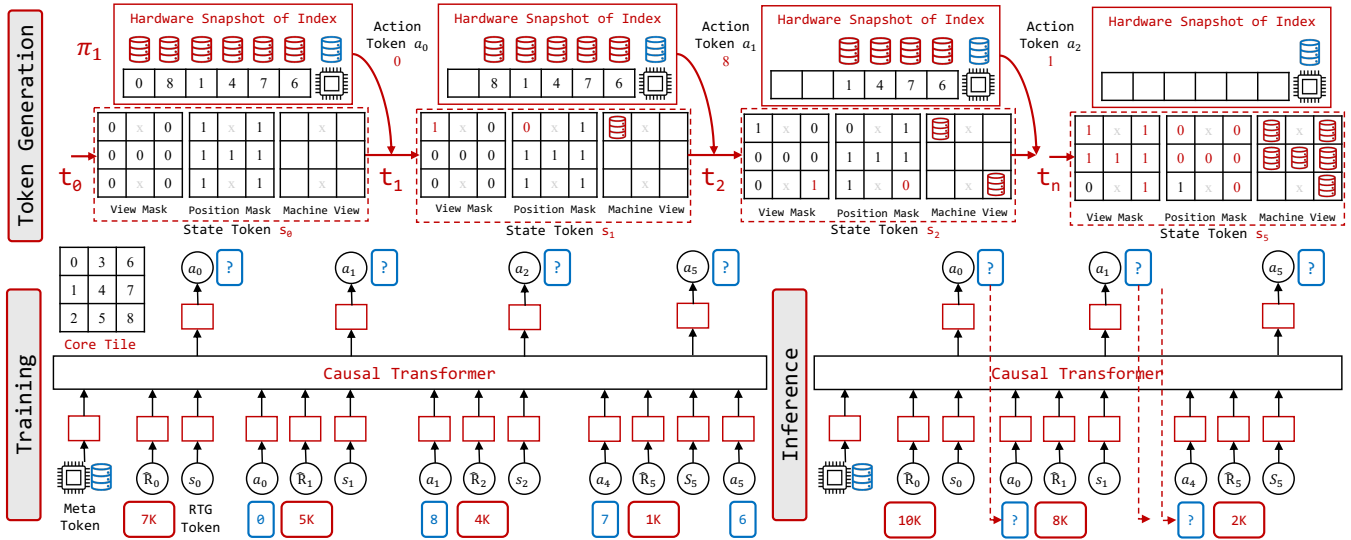


Figure 9: P-MOSS’s Learned Component.

DT in P-MOSS. Refer to the Training and Inference phases in Figure 9 for the DT architecture in P-MOSS. Following the seminal work in [10], the GPT model [59] serves as the backbone for P-MOSS’s DT. GPT replaces the softmax layer of the original Transformer with a causal self-attention mask so that it can be trained in an auto-regressive manner, i.e., by only attending over the previously seen input tokens, in contrast to attending over all the input tokens. P-MOSS feeds a total of $3T+1$ tokens into DT for a single policy in the offline dataset, with T tokens each for the state, action, and return-to-go (RTG) modalities, and an additional meta-token for representing the system-wide view of the NUMA hardware. T refers to the length of the sequence, i.e., the number of index slices to schedule. To obtain the state-token embedding, the state-token is first passed through a convolutional encoder consisting of three convolutional layers, followed by a fully connected layer. To obtain the action, and return-to-go (RTG) embeddings, the respective tokens are passed through separate embedding layers. In addition, P-MOSS learns an embedding for each index slice, and adds the embedding to each token. Once the embeddings are learned, they are passed through the GPT architecture that predicts the next action through autoregressive modeling. Observe that the DT in P-MOSS can be replaced with any autoregressive sequence modeling architecture. However, given the success of Transformers in modeling large sequences, and more importantly, the stability they offer in training, P-MOSS adopts DT.

6.4 Offline Learning

The DT in P-MOSS takes the sequence of state, action, and return-to-go tokens (§ 6.2) as input, and outputs a sequence of predicted actions. The objective of DT is to learn a policy that produces an action distribution conditioned on the sequence of states, actions, and return-to-go tokens.

Training Loop. Figure 9 (Training) illustrates the training of DT in P-MOSS. During the training phase, DT processes each scheduling policy along with the corresponding Hardware Snapshot of the index in the offline dataset, and produces the sequence of input

tokens: state, action, return-to-go, and meta tokens. At a given Time t , DT takes into account the most recent K triplets: state, action, and return-to-go tokens, and predicts the next action a_{t+1} , i.e., the scheduling policy for a particular index slice. K refers to the context length of DT. The meta token is introduced at the final time-step, because the system-wide view of the hardware can only be obtained after all index slices have been scheduled. During training, at Time t_0 , the return-to-go token for a particular policy is initialized to the query throughput that the policy yields. We train P-MOSS’s DT in a supervised manner, where the objective is to align the predicted actions with the actions present in the offline dataset, using the cross-entropy loss. This supervised approach makes the training of the RL agent stable and scalable, in contrast to the traditional Bellman’s Equation-based RL objective that can be brittle depending on the hyper-parameter tuning [10].

Inference. Figure 9 (Inference) illustrates how DT P-MOSS’s DT infers a new scheduling policy. During the inference phase, it initializes the return-to-go token at Time t_0 to the desired query throughput. In P-MOSS, this is set to $1.1\times$, the maximum throughput observed in the offline dataset. P-MOSS also sets the initial state token accordingly. Both the state and return-to-go token are fed into DT that, in turn, generates the first action, i.e., the scheduling policy for the first index slice. P-MOSS observes the recent Hardware Snapshots of the main memory index to obtain the consequent state and reward, following the predicted action. Both the state and the return-to-go token, along with the predicted action are fed back to DT to predict the next action, i.e., the scheduling policy for the next index slice. This process repeats until all the scheduling policy for all the index slices are rolled out.

7 EVALUATION

P-MOSS trains a Decision Transformer on the Hardware Snapshots of a main-memory index collected under various scheduling policies, and learns a novel scheduling policy conditioned on a desired return. In this section, we compare the performance of P-MOSS in

terms of query throughput against the competing baselines. Precisely, we want to answer the following questions:

- How does P-MOSS perform across different CPU vendors, e.g., the Intel, AMD and ARM processors (Addressing Goal 1 of § 2)?
- How does P-MOSS perform in different NUMA architectures, i.e., the COD (cluster on die) or sub-NUMA cluster (SNC) architecture in Intel processors, and the chiplet architecture (Addressing Goal 2 of § 2)?
- How does P-MOSS perform for various query workloads (Addressing Goals 3 & 4 of § 2)?
- How does P-MOSS perform for different indexes?
- How does P-MOSS perform on unseen NUMA machines, and query workloads?

The next sections present the experimental settings and the results of our investigation to answer each of these questions.

7.1 Experimental Settings

Testbed. We evaluate P-MOSS on a diverse set of NUMA machines ranging from different CPU vendors with different NUMA architectures. The details of the NUMA machines are as follows.

1. **Intel Skylake X:** This is a 4 Socket 92 ($\times 2$) core machine running on Ubuntu 22.04. Sub-NUMA Clustering (SNC) is enabled for this machine, i.e., each Socket is divided into 2 NUMA domains. The respective size of L1-D, L1-I, L2, and LLC cache are 3MB, 3MB, 96MB and 132MB. The CPU clock frequency is 2.7 GHz.
2. **AMD EPYC Milan (4NPS):** This is a dual socket 64 ($\times 2$) core machine running Ubuntu 22.04 on a CloudLab [16] r6525 node. The processor is an AMD EPYC 7543 series, where the BIOS setting for NPS (NUMA Per Socket) is set to 4, i.e., each Socket is divided into 4 NUMA domains.
3. **NVIDIA H200 Grace Hopper:** It features a single socket 72 ($\times 1$) core machine running Ubuntu 22.04 on a CloudLab [16] nvidiagh node. The processor is based on ARM’s Neoverse V2 architecture.
4. **Intel Sandy Bridge:** This is a 4 socket 32 ($\times 2$) core machine running Ubuntu 22.04 on a CloudLab [16] d820 node. The processor is an Intel Xeon E5-4620 processor. It does not support Sub-NUMA clustering (SNC) or Cluster On Die (COD) technology.
5. **AMD EPYC Milan (1NPS):** This is a dual socket 64 ($\times 2$) core machine running Ubuntu 22.04 on a CloudLab [16] r6525 node. The processor is an AMD EPYC 7543 series, where the BIOS setting for NPS (NUMA Per Socket) is set to default (=1).

Baselines. We compare P-MOSS with the following baselines. The OS baselines do not assume any logical partitioning of the index. The other baselines assume that the index is logically partitioned into index slices. Automatic NUMA balancing is enabled for P-MOSS and all the baselines.

1. **OS Default (OS:D).** The OS handles the data placement and core scheduling. In Linux, the default NUMA memory policy is *local*, i.e., memory is allocated on the local NUMA node of the core that initiates the memory allocation request [51]. By default, a query can be executed on any of the cores.
2. **OS Interleave (OS:I).** The OS allocates memory in an interleaved fashion. The core scheduling follows the default OS policy.
3. **Shared Everything-NUMA (SE:N)** [54]. Data is placed following a NUMA-aware policy, i.e., index slices with adjacent key

ranges are allocated on the same NUMA node. The OS handles the core scheduling.

4. **Shared Nothing-NUMA (SN:N)** [54]. The data placement follows the Shared Everything-NUMA strategy. The core scheduling maintains the data affinity of the index slice, i.e., a query can only be scheduled on one of the local cores where the data of the corresponding index slice resides.
5. **Shared Nothing-Thread (SN:T).** Both the data placement and core scheduling are NUMA-aware following a Shared Nothing (SN) strategy [54]. A query can only be scheduled on the designated core reserved for the particular index slice that the query accesses. The schedules learned by P-MOSS falls in this category.
 - 5.1. **Grouped.** Index slices with adjacent key ranges are allocated in the same NUMA node and are scheduled in nearby cores.
 - 5.2. **Spread.** Index slices with adjacent key ranges are spread across all the NUMA nodes.
 - 5.3. **Mixed.** Following [54], this Shared-Nothing strategy maintains a middle ground between the two extreme strategies, Grouped and Spread.
 - 5.4. **Random.** This Shared-Nothing strategy does not explicitly abide by any NUMA-aware heuristic. Rather, data placement and core scheduling are done randomly generating a checkerboard pattern.

P-MOSS Configurations. The system component of P-MOSS integrates the main memory B^+ -Tree implementation in [69, 70] and the 2D R-Tree implementation in [21]. The B^+ -Tree implementation follows the optimistic lock coupling (OLC) approach for concurrent operations. The B^+ -Tree leaf node can hold a maximum of 255 entries. The minimum and maximum fanouts of the 2D R-Tree are set to 20 and 50, respectively. For profiling purposes, we integrate the Intel PCM [24] and a C++ wrapper for Linux Perf Event API [37] to read the hardware statistics off the PMU hardware counters in real time. For both the B^+ -Tree and the R-Tree, the number of index slices are set to 256. The scheduling decision of P-MOSS involves allocating cores and IMCs for these 256 index slices.

P-MOSS’s DT implementation is based on [10, 35]. We set the number of layers, attention heads, and embedding size to 6, 8, and 128, respectively. The context length of DT is set to 256, equaling the number of index slices. For a particular query workload and data distribution on a given hardware, we set the desired objective of P-MOSS to equal $2\times$ the best throughput observed in the dataset matching the same context. It takes approximately 18 CPU hours in the AMD Milan (4NPS) server to train P-MOSS’s DT and reach a training accuracy of over 95%. The inference takes up to 1 CPU minute for unseen workloads and hardware platforms on the same server.

7.2 Overall Performance

We examine P-MOSS’s performance against the competing baselines for a B^+ -Tree across all five testbed servers. The goal is to highlight the varying performance characteristics of the same scheduling strategy across different CPU vendors and NUMA architectures. We evaluate P-MOSS on the YCSB benchmark [12] with 30M initial records. Each record consists of a 64 bit key and a 64 bit value. The query workload consists of 50% reads and 50% writes, and follows a Zipfian distribution with the Zipfian constant set to 0.99.

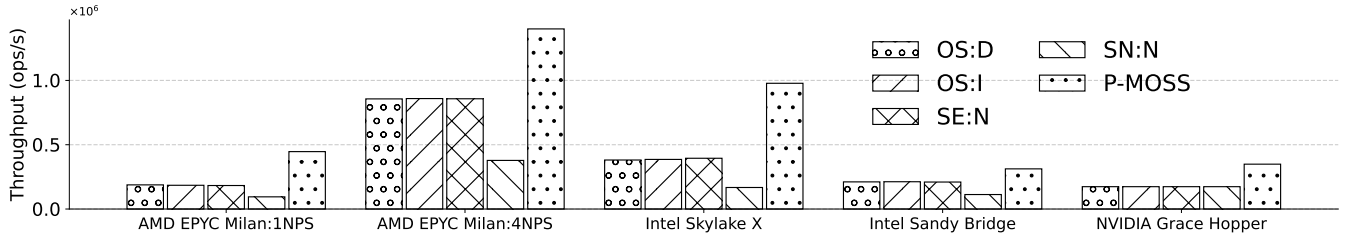


Figure 10: P-MOSS vs OS baselines on 50% Read-Write YCSB workload.

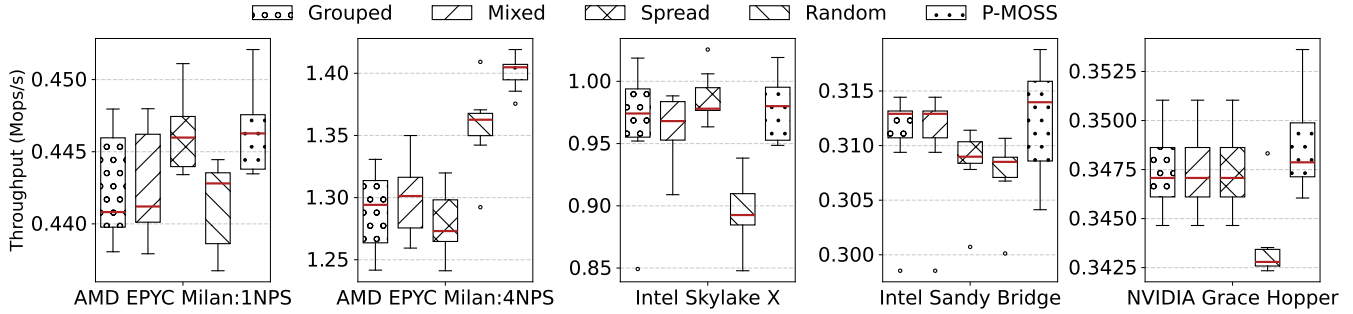


Figure 11: P-MOSS vs SN:T baselines on 50% Read-Write YCSB workload.

We start by showing P-MOSS’s performance against the OS baselines (OS:D, OS:I) and NUMA-aware scheduling strategies (SE:N, SN:N) in Figure 10. Note that both SE:N and SN:N only place index data in a NUMA-aware manner. P-MOSS outperforms all these approaches across all five servers. On average, the learned schedule of P-MOSS achieves a speedup of 4.2 \times over the best performing baseline. Among the baselines, there is no single scheduling strategy that dominates others across servers. For example, the interleaved strategy of OS (OS:I) performs the best for the AMD EPYC Milan (4NPS) and Intel Sandy Bridge server. The Shared Everything NUMA (SE:N) performs best for Intel Skylake X, while the default OS strategy performs best for AMD EPYC Milan (1NPS). For AMD servers, P-MOSS’s performance gain over the OS baselines can be attributed to a reduced number of data cache fills from a remote socket’s cache and memory. P-MOSS also reduces the number of data cache fills from an external (off-chip) cache that is on the same socket. For the Intel servers, P-MOSS reduces the number of remote memory accesses, significantly minimizing the latency of cache and memory stalls. Aside from the remote cache and memory accesses, P-MOSS’s learned schedule also improves the DTLB cache behavior of the B⁺-Tree and reduces the number of executed instructions.

The performance gap between P-MOSS and the SE:N, SN:N strategies show the importance of *compute selection* especially in the context of modern NUMA servers. The SE:N strategy shows a decrease of 1.5 \times in performance over P-MOSS in our oldest server, i.e., Intel Sandy Bridge. The gap widens upto 2.5 \times for the modern processors, i.e., Intel Skylake X and AMD EPYC Milan. This claim is further validated by the performance gap of 2 \times between P-MOSS and the baselines for NVIDIA Grace Hopper that is a single-socket server with a single NUMA node. The only difference between the baselines and P-MOSS lies in how the cores are scheduled to execute index operations for certain index slices. For NVIDIA Grace Hopper, P-MOSS improves the cache efficiency of the B⁺-Tree, and reduces the number of bus, memory accesses. This showcases the

generalization capability of P-MOSS’s PMU-centric learned agent. Depending on the scenario, P-MOSS is able to optimize different criteria and learn better scheduling policies.

Later in Figure 11, we evaluate the performance of P-MOSS’s learned schedule against the SN:T strategies, that take both core scheduling and data placement into account. P-MOSS not only learns scheduling strategies that exhibit robust performance across all the testbed NUMA servers, it also dominates the baselines. For example, in AMD EPYC Milan (4NPS), P-MOSS outperforms the closest competitor by 1.1 \times . Similar to the OS baselines, no single SN:T strategy exhibits robust performance across the NUMA servers for the read-write workload. For Intel processors, i.e., Skylake X and Sandy Bridge, the Grouped strategy yields better throughput. To the contrary, the chiplet-based AMD processors prefer a more randomized strategy. For example, the Spread and Random strategies are the closest competitors to P-MOSS in AMD EPYC Milan processors.

7.3 Different Query Workloads

This section examines the performance of P-MOSS for the B⁺-Tree on two important workloads: point lookup and scan workloads. The point lookup workload consists of 100% point lookups that follow a uniform distribution. The scan workload consists of 95% scans and 5% inserts that follow a Zipfian distribution. The selectivity of each range scan is uniformly distributed ranging up to 0.001%. We evaluate P-MOSS against the competing baselines for the point lookup workload in Figures 12 and 13. Later in Figures 14 and 15, we evaluate P-MOSS for the scan workload.

Point Lookup Workload: For point lookup, P-MOSS outperforms the OS baselines and the SE:N, SN:N strategies by 3.75 \times on average (cf. Figure 12). For AMD EPYC Milan (4 NPS), the OS’s interleaved strategy performs the worst, while the same approach is the closest competitor when the NPS BIOS setting of AMD EPYC Milan is set to 1. This aligns with our previous observation of no one strategy being optimal for all the cases, i.e., workloads.

Among the SN:T strategies, the learned schedule of P-MOSS maintains its robust performance across all our testbed servers (cf. Figure 13). For AMD EPYC Milan and Intel Sandy Bridge, P-MOSS outperforms the closest competitor by 1.1 \times . For Intel Skylake X, the learned schedule of P-MOSS shows minimal degradation. Aligned with our earlier observation for read-write workloads, a randomized strategy thrives in AMD EPYC Milan (4NPS) for point lookup workload as well. The Intel processors yield better throughput for the Grouped strategy.

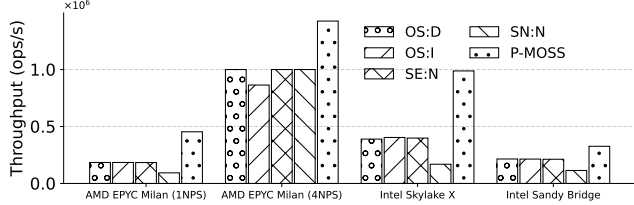


Figure 12: P-MOSS vs OS baselines on YCSB point lookup workload.

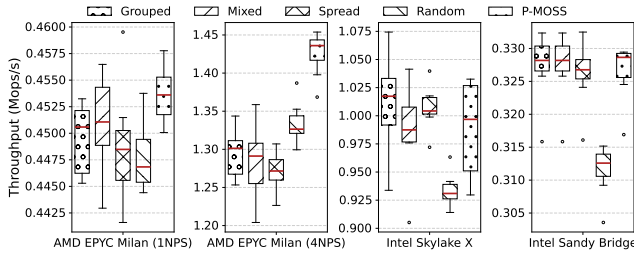


Figure 13: P-MOSS vs SN:T baselines on YCSB point lookup workload

Scan Workload: For the scan workload, P-MOSS outperforms the default OS strategy by 2 \times (cf. Figure 14). The gap is the least in our earliest server, i.e., Intel Sandy Bridge server at 1.5 \times aligning with the same observation for the read-write workload. The gap widens up to 2.4 \times for the Intel Skylake X and AMD EPYC Milan processors. In comparison to the variable performance of the SN:T strategies across different machines, P-MOSS’s schedule remains robust (cf. Figure 15).

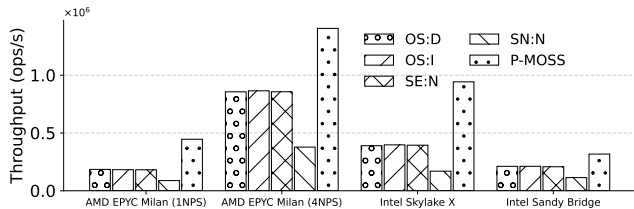


Figure 14: P-MOSS vs OS baselines on scan workload.

7.4 Applicability to Other Index Types

We evaluate the performance of P-MOSS on a different index, mainly, the 2D R-Tree [22]. The experiments are run on the Intel Skylake X server for the OSM US Northeast [49] dataset, with 50M initial records. The dataset contains real points of interest (POIs) of US NorthEast region in the form of 64-bit keys. The query workload comprises 100% uniformly distributed range scans. Figure 16 gives P-MOSS’s performance against the competing baselines.

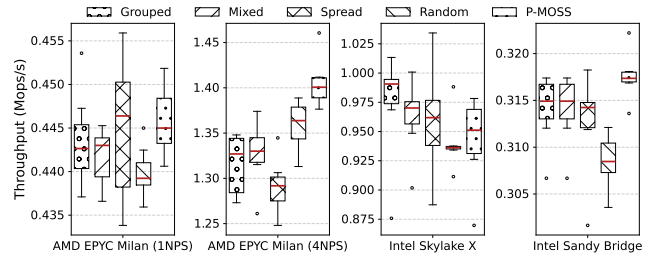


Figure 15: P-MOSS vs SN:T baselines on scan workload

On average, P-MOSS achieves a speedup of 2.7 \times over the competing baselines that include the OS, SE:N, SN:N, and SN:T strategies. Among the SN:T baselines, the Grouped strategy is the closest competitor to P-MOSS. P-MOSS outperforms the Grouped strategy by 1.2 \times . The performance gap significantly widens up to 3 \times for the other SN:T strategies, e.g., as in the Mixed approach. One observation is that the performance gap between P-MOSS and the SN:T baselines is wider for the R-Tree index compared to P-MOSS’s performance for B⁺-Tree index. As the experiments are run on a 2D R-Tree, this introduces another dimension in the key space over a B⁺-Tree. This in turn expands the design space of the scheduling strategies, and hence the potential for finding better schedules, and hence better performance improvements.

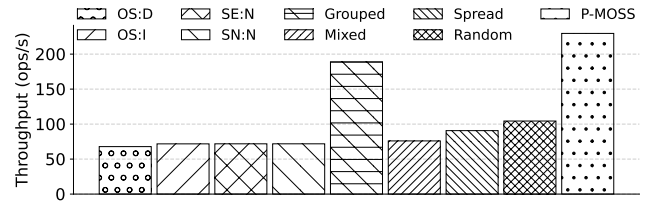


Figure 16: P-MOSS vs OS and SN:T baselines for R-Tree index.

7.5 Generalization

This section examines the performance of P-MOSS in situations where the query workloads, data distribution or hardware platforms are not known beforehand. We evaluate if P-MOSS can generalize beyond the data that it has been trained on and can keep up with the competing baselines. Figures 17 and 18 present the performance of P-MOSS in four such cases. Notice that P-MOSS does not log any scheduling policy in its offline dataset pertaining to the the query workloads, datasets, or the hardware platforms discussed below.

Unseen Query Workload. Figures 17a, 18a give the performance of P-MOSS on a query workload that consists of 50% point lookups and 50% scans. The query distribution follows a Zipfian distribution and is evaluated on the AMD EPYC Milan (4NPS) server. P-MOSS outperforms the OS interleaved strategy by 2.5 \times . Contrary to the previous observations, the Grouped strategy dominates over the Random strategy for the stated workload in the AMD EPYC Milan (4NP) server. P-MOSS outperforms the SN:T strategies by 1.1 \times .

Unseen Data Distribution. Figures 17b, 18b give the performance of P-MOSS on the OSM dataset [29, 60] with 30M initial records. The data distribution of OSM differs from the YCSB benchmark. We use the default 50% read-write workload in § 7.2 and run the experiments on AMD EPYC Milan (4NPS) server. On average,

P-MOSS outperforms the OS baselines, and the SE:N, SN:N, SN:T strategies by 1.3 \times .

Unseen Hardware Platforms. Figures 17c, 18c give the performance of P-MOSS on a 16-core AMD EPYC Rome processor, different from the AMD EPYC Milan processors in our testbed. Each Core Complex Die (CCD) in a Rome NUMA socket contains 2 separate Core Complexes (CCX), each having 4 cores. This results in variable core-to-core latency between the cores in different CCXs. In contrast, each CCD in Milan sockets have a unified CCX with 8 cores. P-MOSS outperforms the OS baselines and performs almost as good as the Grouped strategy on this hardware.

Figures 17d, 18d give the performance of P-MOSS on an Intel Skylake X server with 4 NUMA sockets and 4 NUMA nodes. Unlike the Skylake server in our testbed, this hardware platform does not employ any Sub-NUMA clustering (SNC). Hence, it differs in the NUMA architecture and the available number of NUMA nodes. The evaluation is performed on the default read-write workload consisting of 50% point lookups and 50% inserts. P-MOSS outperforms all the baselines on this particular unseen hardware as well.

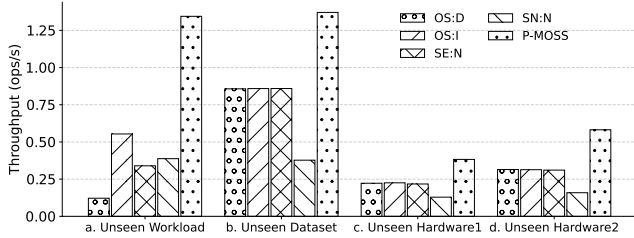


Figure 17: P-MOSS vs OS baselines on unseen workloads and hardware.

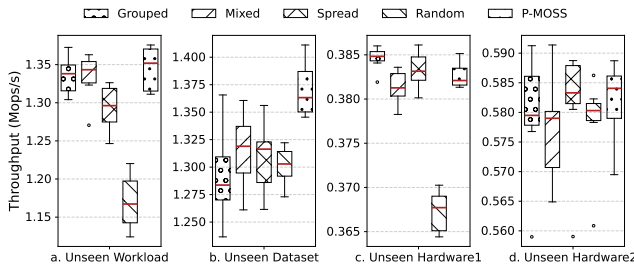


Figure 18: P-MOSS vs SN:T baselines on unseen workloads and hardware.

8 RELATED WORK

NUMA-awareness in Main Memory DBMSs. Prior work on NUMA includes stand-alone NUMA-aware query operators, synchronization, and scheduling strategies. Stream join [65], sort-merge join [1, 41], hash join [6, 36], radix join [62] are examples of existing work on standalone NUMA-aware query operators. A different body of work in NUMA delves into the synchronization primitives, e.g., designing NUMA-friendly locks [9, 28, 42] and concurrent data structures [8]. The NUMA related studies that probably pose the closest resemblance to P-MOSS is NUMA-aware query scheduling [38, 53, 54, 57, 58, 67]. The morsel-driven query scheduling framework of both HyPer [38] and Umbra [67] stores relations as morsels (data fragments), and uniformly distributes them over

the NUMA sockets. Each worker thread operates on morsels local to it, and writes the results to the local NUMA socket. The NUMA-aware query scheduling framework in SAP HANA [57, 58] adaptively partitions tables, and locates them in appropriate NUMA sockets to balance the load across the NUMA sockets. It tracks the CPU and memory bandwidth utilization history of tasks, tables, and the NUMA sockets. All of these works are centered on relational tables, and do not consider query scheduling over main-memory indexes. Beyond the realm of DRAM, NUMA has also been studied in the context of Persistent Memory (PM) [13, 68].

Temporal Query Scheduling. Besides the NUMA-aware query scheduling policies, there exists a different body of work on temporal query scheduling that does not explicitly handle NUMA awareness. These works include both heuristic-driven [52] and learned [44, 61] strategies.

Index Clustering. There exists a different line of work on clustering and declustering tree index nodes, e.g., B⁺-Tree [56, 63] and R-Tree [15, 27, 32] to improve query performance. However, these proposed works address varying contexts, different machine architecture, and disk-based indexes. Buzzard [43] is another related work that proposes an in-memory NUMA-aware indexing technique that applies a heuristic-based adaptive data partitioning scheme to distribute a prefix-tree-based index across the NUMA system to optimize remote memory accesses. For robust performance, [7] partitions the hardware resources and assigns them index instances to isolate index operations. Unlike P-MOSS, it ignores the spatial aspect of the scheduled index operations.

9 CONCLUSION

In this paper, we present P-MOSS, a Performance Monitoring Unit (PMU)-driven learned scheduling framework that improves the query processing in main memory indexes on modern multi-core NUMA servers. The learning process of P-MOSS accommodates the Offline RL paradigm, enabling it to gather the behavioral knowledge of the main memory indexes for various data distributions, query workloads, and hardware architectures from the PMU hardware counters, in the form of an offline dataset. P-MOSS generalizes beyond the observed samples in the gathered offline dataset, and learns a better scheduling policy. Experiments on both the B⁺-Tree and the R-Tree in diverse settings illustrate that P-MOSS improves the index performance upto 6 \times . Overall, the performance results of P-MOSS suggests that the hardware performance counters gathered from PMU of the hardware coupled with Offline RL can guide DBMS optimization tasks. While this paper is presented in the context of spatial scheduling over main-memory indexes, the techniques in this paper can be generalized beyond learning spatial scheduling policies to designing DBMS optimizations.

10 ACKNOWLEDGEMENTS

Walid G. Aref acknowledges the support of the National Science Foundation under Grant Number IIS-1910216.

REFERENCES

- [1] Martina-Cezara Albutiu, Alfons Kemper, and Thomas Neumann. 2012. Massively Parallel Sort-Merge Joins in Main Memory Multi-Core Database Systems. *VLDB* 5, 10 (2012), 1064–1075. <https://doi.org/10.14778/2336664.2336678>
- [2] AMD. 2024. *AMD EPYC™ Processors 7003 Series*. Retrieved October 18, 2024 from <https://www.amd.com/en/products/processors/server/epyc/7003-series.html>
- [3] AMD. 2024. *AMD Performance Monitors*. Retrieved July 3, 2024 from <https://docs.amd.com/r/en-US/ug1085-zynq-ultrascale-trm/Performance-Monitors>
- [4] Christoph Anneser, Andreas Kipf, Huanchen Zhang, Thomas Neumann, and Alfons Kemper. 2022. Adaptive Hybrid Indexes. In *SIGMOD*. ACM, 1626–1639. <https://doi.org/10.1145/3514221.3526121>
- [5] ARM. 2024. *ARM Performance Monitors*. Retrieved July 3, 2024 from <https://developer.arm.com/documentation/ddi0433/c/performance-monitoring-unit>
- [6] Cagri Balkesen, Gustavo Alonso, Jens Teubner, and M. Tamer Özsu. 2013. Multi-Core, Main-Memory Joins: Sort vs. Hash Revisited. *VLDB* 7, 1 (2013), 85–96. <https://doi.org/10.14778/2732219.2732227>
- [7] Tiemo Bang, Ismail Oukid, Norman May, Iliia Petrov, and Carsten Binnig. 2020. Robust Performance of Main Memory Data Structures by Configuration. In *SIGMOD*. ACM, 1651–1666. <https://doi.org/10.1145/3318464.3389725>
- [8] Irina Calciu, Siddhartha Sen, Mahesh Balakrishnan, and Marcos K. Aguilera. 2017. Black-box Concurrent Data Structures for NUMA Architectures. In *ASPLOS*. ACM, 207–221. <https://doi.org/10.1145/3037697.3037721>
- [9] Milind Chhabbi, Michael W. Fagan, and John M. Mellor-Crummey. 2015. High performance locks for multi-level NUMA systems. In *PoPP*. ACM, 215–226. <https://doi.org/10.1145/2688500.2688503>
- [10] Lili Chen, Kevin Lu, Aravind Rajeswaran, Kimin Lee, Aditya Grover, Michael Laskin, Pieter Abbeel, Aravind Srinivas, and Igor Mordatch. 2021. Decision Transformer: Reinforcement Learning via Sequence Modeling. In *NeurIPS*. 15084–15097. <https://proceedings.neurips.cc/paper/2021/hash/7f489f642a0ddb10272b5c31057f0663-Abstract.html>
- [11] Douglas Comer. 1979. The Ubiquitous B-Tree. *ACM Comput. Surv.* 11, 2 (1979), 121–137. <https://doi.org/10.1145/356770.356776>
- [12] Brian F. Cooper, Adam Silberstein, Erwin Tam, Raghu Ramakrishnan, and Russell Sears. 2010. Benchmarking cloud serving systems with YCSB. In *SoCC*. ACM, 143–154. <https://doi.org/10.1145/1807128.1807152>
- [13] Björn Daase, Lars Jonas Bollmeier, Lawrence Benson, and Tilmann Rabl. 2021. Maximizing Persistent Memory Bandwidth Utilization for OLAP Workloads. In *SIGMOD*. ACM, 339–351. <https://doi.org/10.1145/3448016.3457292>
- [14] Reetuparna Das, Rachata Ausavarungnirun, Onur Mutlu, Akhilesh Kumar, and Mani Azimi. 2013. Application-to-core mapping policies to reduce memory system interference in multi-core systems. In *HPCA*. IEEE Computer Society, 107–118. <https://doi.org/10.1109/HPCA.2013.6522311>
- [15] Ajit A. Diwan, Sanjeeva Rane, S. Seshadri, and S. Sudarshan. 1996. Clustering Techniques for Minimizing External Path Length. In *VLDB*. Morgan Kaufmann, 342–353.
- [16] Dmitry Duplyakin, Robert Ricci, Aleksander Maricq, Gary Wong, Jonathon Duerig, Eric Eide, Leigh Stoller, Mike Hibler, David Johnson, Kirk Webb, Aditya Akella, Kuang-Ching Wang, Glenn Ricart, Larry Landweber, Chip Elliott, Michael Zink, Emmanuel Cecchet, Snigdhaswin Kar, and Prabodh Mishra. 2019. The Design and Operation of CloudLab. In *USENIX*. USENIX Association, 1–14. <https://www.usenix.org/conference/atc19/presentation/duplyakin>
- [17] Franz Faerber, Alfons Kemper, Per-Åke Larson, Justin J. Levandoski, Thomas Neumann, and Andrew Pavlo. 2017. Main Memory Database Systems. *Found. Trends Databases* 8, 1–2 (2017), 1–130. <https://doi.org/10.1561/19000000058>
- [18] Scott Fujimoto and Shixiang Shane Gu. 2021. A Minimalist Approach to Offline Reinforcement Learning. In *NeurIPS*. 20132–20145. <https://proceedings.neurips.cc/paper/2021/hash/a8166da05c5a094f7dc03724b41886e5-Abstract.html>
- [19] Scott Fujimoto, David Meger, and Doina Precup. 2019. Off-Policy Deep Reinforcement Learning without Exploration. In *ICML (Proceedings of Machine Learning Research)*, Vol. 97. PMLR, 2052–2062. <http://proceedings.mlr.press/v97/fujimoto19a.html>
- [20] Goetz Graefe, Stratos Idreos, Harumi A. Kuno, and Stefan Manegold. 2010. Benchmarking Adaptive Indexing. In *TPCTC (Lecture Notes in Computer Science)*, Vol. 6417. Springer, 169–184. https://doi.org/10.1007/978-3-642-18206-8_13
- [21] Tu Gu, Kaiyu Feng, Gao Cong, Cheng Long, Zheng Wang, and Sheng Wang. 2023. The RLR-Tree: A Reinforcement Learning Based R-Tree for Spatial Data. *Proc. ACM Manag. Data* 1, 1 (2023), 63:1–63:26.
- [22] Antonin Guttman. 1984. R-Trees: A Dynamic Index Structure for Spatial Searching. In *SIGMOD*. ACM Press, 47–57.
- [23] Benjamin Hilprecht, Carsten Binnig, and Uwe Röhm. 2020. Learning a Partitioning Advisor for Cloud Databases. In *SIGMOD*. ACM, 143–157. <https://doi.org/10.1145/3318464.3389704>
- [24] Intel. 2024. *Intel PCM*. Retrieved July 3, 2024 from <https://github.com/intel/pcm>
- [25] Intel. 2024. *Intel Performance Monitoring Event*. Retrieved July 3, 2024 from <https://github.com/intel/perfmon>
- [26] Intel. 2024. *Intel Skylake Processors*. Retrieved October 18, 2024 from <https://ark.intel.com/content/www/us/en/ark/products/codename/37572/products-formerly-skylake.html>
- [27] Ibrahim Kamel and Christos Faloutsos. 1992. Parallel R-trees. In *SIGMOD Conference*. ACM Press, 195–204.
- [28] Sanidhya Kashyap, Changwoo Min, and Taesoo Kim. 2017. Scalable NUMA-aware Blocking Synchronization Primitives. In *ATC*. USENIX Association, 603–615. <https://www.usenix.org/conference/atc17/technical-sessions/presentation/kashyap>
- [29] Andreas Kipf, Ryan Marcus, Alexander van Renen, Mihail Stoian, Alfons Kemper, Tim Kraska, and Thomas Neumann. 2019. SOSD: A Benchmark for Learned Indexes. *CoRR* abs/1911.13014 (2019). arXiv:1911.13014 <http://arxiv.org/abs/1911.13014>
- [30] Thomas Kissinger, Benjamin Schlegel, Dirk Habich, and Wolfgang Lehner. 2013. QPPT: Query Processing on Prefix Trees. In *CIDR*. www.cidrdb.org. http://cidrdb.org/cidr2013/Papers/CIDR13_Paper3.pdf
- [31] Ilya Kostrikov, Ashvin Nair, and Sergey Levine. 2022. Offline Reinforcement Learning with Implicit Q-Learning. In *ICLR*. OpenReview.net. <https://openreview.net/forum?id=68n2s9ZJWF8>
- [32] Nick Koudas, Christos Faloutsos, and Ibrahim Kamel. 1996. Declustering Spatial Databases on a Multi-Computer Architecture. In *EDBT (Lecture Notes in Computer Science)*, Vol. 1057. Springer, 592–614.
- [33] Sanjay Krishnan, Zongheng Yang, Ken Goldberg, Joseph M. Hellerstein, and Ion Stoica. 2018. Learning to Optimize Join Queries With Deep Reinforcement Learning. *CoRR* abs/1808.03196 (2018). arXiv:1808.03196 <http://arxiv.org/abs/1808.03196>
- [34] Aviral Kumar, Aurick Zhou, George Tucker, and Sergey Levine. 2020. Conservative Q-Learning for Offline Reinforcement Learning. In *NeurIPS*. <https://proceedings.neurips.cc/paper/2020/hash/0d2b2061826a5df322116a5085a6052-Abstract.html>
- [35] Yao Lai, Jinxin Liu, Zhentao Tang, Bin Wang, Jianye Hao, and Ping Luo. 2023. ChipFormer: Transferable Chip Placement via Offline Decision Transformer. In *ICML (PMLR)*, Vol. 202. PMLR, 18346–18364.
- [36] Harald Lang, Viktor Leis, Martina-Cezara Albutiu, Thomas Neumann, and Alfons Kemper. 2013. Massively Parallel NUMA-aware Hash Joins. In *IMDM*. 1–12. <http://www-db.in.tum.de/other/imdm2013/papers/Lang.pdf>
- [37] Viktor Leis. 2024. *An easy-to-use, header-only C++ wrapper for Linux' perf event API*. Retrieved July 3, 2024 from <https://github.com/viktorleis/perfevent/tree/master>
- [38] Viktor Leis, Peter A. Boncz, Alfons Kemper, and Thomas Neumann. 2014. Morsel-driven parallelism: a NUMA-aware query evaluation framework for the many-core age. In *SIGMOD*. ACM, 743–754. <https://doi.org/10.1145/2588555.2610507>
- [39] Sergey Levine, Aviral Kumar, George Tucker, and Justin Fu. 2020. Offline Reinforcement Learning: Tutorial, Review, and Perspectives on Open Problems. *CoRR* abs/2005.01643 (2020). arXiv:2005.01643 <https://arxiv.org/abs/2005.01643>
- [40] Guoliang Li, Xuanhe Zhou, Shifu Li, and Bo Gao. 2019. QTune: A Query-Aware Database Tuning System with Deep Reinforcement Learning. *VLDB* 12, 12 (2019), 2118–2130. <https://doi.org/10.14778/3352063.3352129>
- [41] Yinan Li, Ippokratis Pandis, René Müller, Vijayshankar Raman, and Guy M. Lohman. 2013. NUMA-aware algorithms: the case of data shuffling. In *CIDR*. www.cidrdb.org. http://cidrdb.org/cidr2013/Papers/CIDR13_Paper121.pdf
- [42] Jean-Pierre Lozi, Florian David, Gaël Thomas, Julia Lawall, and Gilles Muller. 2016. Fast and Portable Locking for Multicore Architectures. *ACM Trans. Comput. Syst.* 33, 4 (2016), 13:1–13:62. <https://dl.acm.org/citation.cfm?id=2845079>
- [43] Lukas M. Maas, Thomas Kissinger, Dirk Habich, and Wolfgang Lehner. 2013. BUZZARD: a NUMA-aware in-memory indexing system. In *SIGMOD Conference*. ACM, 1285–1286.
- [44] Hongzi Mao, Malte Schwarzkopf, Shaileshh Bojja Venkatakrisnan, Zili Meng, and Mohammad Alizadeh. 2019. Learning scheduling algorithms for data processing clusters. In *SIGCOMM*. ACM, 270–288. <https://doi.org/10.1145/3341302.3342080>
- [45] Ryan Marcus, Parimarjan Negi, Hongzi Mao, Nesime Tatbul, Mohammad Alizadeh, and Tim Kraska. 2021. Bao: Making Learned Query Optimization Practical. In *SIGMOD*. ACM, 1275–1288. <https://doi.org/10.1145/3448016.3452838>
- [46] Ryan Marcus, Parimarjan Negi, Hongzi Mao, Chi Zhang, Mohammad Alizadeh, Tim Kraska, Olga Papaemmanouil, and Nesime Tatbul. 2019. Neo: A Learned Query Optimizer. *VLDB* 12, 11 (2019), 1705–1718. <https://doi.org/10.14778/3342263.3342644>
- [47] Azalia Mirhoseini, Anna Goldie, Mustafa Yazgan, Joe Wenjie Jiang, Ebrahim M. Songhori, Shen Wang, Young-Joon Lee, Eric Johnson, Omkar Pathak, Azade Nazi, Jiwoo Pak, Andy Tong, Kavya Srinivasa, William Hang, Emre Tuncer, Quoc V. Le, James Laudon, Richard Ho, Roger Carpenter, and Jeff Dean. 2021. A graph placement methodology for fast chip design. *Nat.* 594, 7862 (2021), 207–212.
- [48] NVIDIA. 2014. *NVIDIA GH200 Grace Hopper Superchip*. Retrieved October 18, 2024 from <https://www.nvidia.com/en-us/data-center/grace-hopper-superchip/>
- [49] OpenStreetMap. 2024. *OpenstreetMap US NorthEast Dataset*. Retrieved July 3, 2024 from <https://download.geofabrik.de/north-america/us-northeast.html>
- [50] Jennifer Ortiz, Magdalena Balazinska, Johannes Gehrke, and S. Sathya Keerthi. 2018. Learning State Representations for Query Optimization with Deep Reinforcement Learning. In *DEEM*. ACM, 4:1–4:4. <https://doi.org/10.1145/3209889>

- [51] Linux Man Pages. 2024. *Linux NUMA Memory Policy*. Retrieved July 3, 2024 from https://man7.org/linux/man-pages/man2/set_mempolicy.2.html
- [52] Jignesh M. Patel, Harshad Deshmukh, Jianqiao Zhu, Navneet Potti, Zuyu Zhang, Marc Spehlmann, Hakan Memisoglu, and Saket Saurabh. 2018. Quickstep: A Data Platform Based on the Scaling-Up Approach. *Proc. VLDB Endow.* 11, 6 (2018), 663–676. <https://doi.org/10.14778/3184470.3184471>
- [53] Danica Porobic, Erietta Liarou, Pinar Tözün, and Anastasia Ailamaki. 2014. ATraPos: Adaptive transaction processing on hardware Islands. In *ICDE*. IEEE Computer Society, 688–699. <https://doi.org/10.1109/ICDE.2014.6816692>
- [54] Danica Porobic, Ippokratis Pandis, Miguel Branco, Pinar Tözün, and Anastasia Ailamaki. 2012. OLTP on Hardware Islands. *VLDB* 5, 11 (2012), 1447–1458. <https://doi.org/10.14778/2350229.2350260>
- [55] PostgreSQL. 2024. *Index-Only Scans*. Retrieved October 11, 2024 from <https://www.postgresql.org/docs/current/indexes-index-only-scans.html>
- [56] Sakti Pramanik and Myoung-Ho Kim. 1990. Parallel Processing of Large Node B-Trees. *IEEE Trans. Computers* 39, 9 (1990), 1208–1212.
- [57] Iraklis Psaroudakis, Tobias Scheuer, Norman May, Abdelkader Sellami, and Anastasia Ailamaki. 2015. Scaling Up Concurrent Main-Memory Column-Store Scans: Towards Adaptive NUMA-aware Data and Task Placement. *VLDB* 8, 12 (2015), 1442–1453. <https://doi.org/10.14778/2824032.2824043>
- [58] Iraklis Psaroudakis, Tobias Scheuer, Norman May, Abdelkader Sellami, and Anastasia Ailamaki. 2016. Adaptive NUMA-aware data placement and task scheduling for analytical workloads in main-memory column-stores. *VLDB* 10, 2 (2016), 37–48. <https://doi.org/10.14778/3015274.3015275>
- [59] Alec Radford, Karthik Narasimhan, Tim Salimans, and Ilya Sutskever. 2018. *Improving Language Understanding by Generative Pre-Training*. Technical Report.
- [60] Aneesh Raman, Andy Huynh, Jinqi Lu, and Manos Athanassoulis. 2024. Benchmarking Learned and LSM Indexes for Data Sortedness. In *DBTest*. ACM, 16–22. <https://doi.org/10.1145/3662165.3662764>
- [61] Ibrahim Sabek, Tenzin Samten Ukyab, and Tim Kraska. 2022. LSched: A Workload-Aware Learned Query Scheduler for Analytical Database Systems. In *SIGMOD*. ACM, 1228–1242. <https://doi.org/10.1145/3514221.3526158>
- [62] Stefan Schuh, Xiao Chen, and Jens Dittrich. 2016. An Experimental Comparison of Thirteen Relational Equi-Joins in Main Memory. In *SIGMOD*. ACM, 1961–1976. <https://doi.org/10.1145/2882903.2882917>
- [63] Bernhard Seeger and Per-Åke Larson. 1991. Multi-Disk B-trees. In *SIGMOD Conference*. ACM Press, 436–445.
- [64] Radu Stoica and Anastasia Ailamaki. 2013. Enabling efficient OS paging for main-memory OLTP databases. In *DaMoN*. ACM, 7. <https://doi.org/10.1145/2485278.2485285>
- [65] Jens Teubner and René Müller. 2011. How soccer players would do stream joins. In *SIGMOD*. ACM, 625–636. <https://doi.org/10.1145/1989323.1989389>
- [66] Ashish Vaswani, Noam Shazeer, Niki Parmar, Jakob Uszkoreit, Llion Jones, Aidan N. Gomez, Lukasz Kaiser, and Illia Polosukhin. 2017. Attention is All you Need. In *NeurIPS*. 5998–6008. <https://proceedings.neurips.cc/paper/2017/hash/3f5ee243547dee91fbd053c1c4a845aa-Abstract.html>
- [67] Benjamin Wagner, André Kohn, and Thomas Neumann. 2021. Self-Tuning Query Scheduling for Analytical Workloads. In *SIGMOD*. ACM, 1879–1891. <https://doi.org/10.1145/3448016.3457260>
- [68] Qing Wang, Youyou Lu, Junru Li, and Jiwu Shu. 2021. Nap: A Black-Box Approach to NUMA-Aware Persistent Memory Indexes. In *OSDI*. USENIX Association, 93–111. <https://www.usenix.org/conference/osdi21/presentation/wang-qing>
- [69] Ziqi Wang. 2017. *Index Micro Benchmarks*. Retrieved October 11, 2024 from <https://github.com/wangziqi2016/index-microbench>
- [70] Ziqi Wang, Andrew Pavlo, Hyeontaek Lim, Viktor Leis, Huan Chen Zhang, Michael Kaminsky, and David G. Andersen. 2018. Building a Bw-Tree Takes More Than Just Buzz Words. In *SIGMOD*. ACM, 473–488. <https://doi.org/10.1145/3183713.3196895>
- [71] Petrie Wong, Ziqiang Feng, Wenjian Xu, Eric Lo, and Ben Kao. 2015. TLB misses: The Missing Issue of Adaptive Radix Tree?. In *DaMoN*. ACM, 6:1–6:7. <https://doi.org/10.1145/2771937.2771942>
- [72] Huan Chen Zhang, David G. Andersen, Andrew Pavlo, Michael Kaminsky, Lin Ma, and Rui Shen. 2016. Reducing the Storage Overhead of Main-Memory OLTP Databases with Hybrid Indexes. In *SIGMOD*. ACM, 1567–1581. <https://doi.org/10.1145/2882903.2915222>
- [73] Ji Zhang, Yu Liu, Ke Zhou, Guoliang Li, Zhili Xiao, Bin Cheng, Jiashu Xing, Yangtao Wang, Tianheng Cheng, Li Liu, Minwei Ran, and Zekang Li. 2019. An End-to-End Automatic Cloud Database Tuning System Using Deep Reinforcement Learning. In *SIGMOD*. ACM, 415–432. <https://doi.org/10.1145/3299869.3300085>
- [74] Qinqing Zheng, Amy Zhang, and Aditya Grover. 2022. Online Decision Transformer. In *ICML (Proceedings of Machine Learning Research)*, Vol. 162. PMLR, 27042–27059. <https://proceedings.mlr.press/v162/zheng22c.html>